

Journal of Materials Chemistry A

Accepted Manuscript



This is an *Accepted Manuscript*, which has been through the Royal Society of Chemistry peer review process and has been accepted for publication.

Accepted Manuscripts are published online shortly after acceptance, before technical editing, formatting and proof reading. Using this free service, authors can make their results available to the community, in citable form, before we publish the edited article. We will replace this *Accepted Manuscript* with the edited and formatted *Advance Article* as soon as it is available.

You can find more information about *Accepted Manuscripts* in the [Information for Authors](#).

Please note that technical editing may introduce minor changes to the text and/or graphics, which may alter content. The journal's standard [Terms & Conditions](#) and the [Ethical guidelines](#) still apply. In no event shall the Royal Society of Chemistry be held responsible for any errors or omissions in this *Accepted Manuscript* or any consequences arising from the use of any information it contains.

Cite this: DOI: 10.1039/c0xx00000x

www.rsc.org/xxxxxx

ARTICLE TYPE

Mesocrystal Co_9S_8 hollow sphere anode for high performance lithium ion batteries

Rencheng Jin,^{*a} Junhao Zhou,^a Yanshuai Guan,^a Hong Liu,^a Gang Chen^b

Received (in XXX, XXX) Xth XXXXXXXXX 20XX, Accepted Xth XXXXXXXXX 20XX

DOI: 10.1039/b000000x

Mesocrystal Co_9S_8 with high capacity and good cycle stability (254.9 mAh g^{-1} after 100 cycles at the current density of 100 mA g^{-1}) was prepared through solvothermal method in the presence of hexamethylenetetramine.

Introduction

Lithium ion batteries (LIBs) have been widely used in portable electronic applications¹⁻³ due to the advantages of high energy density, long lifespan and environmental benignity. However, the traditional commercial graphite anode has hindered further development of LIBs with high energy density due to their low specific capacity. To solve the problem, new anode materials including metal oxides/sulfides with higher specific capacities are needed.^{4,5} Among numerous new candidates of anode materials, cobalt sulfides with different stoichiometric composition such as CoS ,⁶ CoS_2 ,⁷ Co_3S_4 ⁸ and Co_9S_8 ⁹ are believed as promising substitution for commercial graphite owing to their high theoretical lithium storage capacity. Unfortunately, these cobalt sulfides usually suffer from rapid capacity fading, low initial coulombic efficiency and poor rate performance, which limits their practical application. This problem may be attributed to the drastic volume change destruction of the electrode during charge/discharge process, similar to the metal oxides.¹⁰⁻¹² Recent years, considerable efforts have been made to address the above issues by designing nanostructured cobalt sulfides with different sizes, shapes and component compositions.^{6, 7, 9, 13} A possible effective route is to construct hollow or porous structure, which shortens Li^+ diffusion pathway, increases electrode/electrolyte contact surface that can provide faster reactions, and accommodates the volume change.^{7, 12, 14, 15}

Herein we present a facile solvothermal method for the growth of Co_9S_8 hollow spheres assembled by mesocrystalline nanoplates with the assistance of hexamethylenetetramine. The Li ion storage performance is tested. The Co_9S_8 hollow spheres present high charge-discharge capacity and good cycling performance. A reversible discharge capacity as high as 254.9 mAh g^{-1} can be delivered after 100 cycles at the current density of 100 mA g^{-1} .

Results and discussion

Fig. 1a shows the XRD pattern of the obtained product after solvothermal treatment. The diffraction peaks can be easily

assigned to the (111), (311), (222), (331), (511), (440), (531), (444), (731), (800) planes of the cubic phase of Co_9S_8 (JCPDS No. 86-2273). The morphology of the product was examined by field emission scanning electron microscopy (FESEM). A large amount of well-defined, hollow microspheres with a diameter of 1-5 μm were formed (Fig. 1b). More details in the magnified SEM image (Fig. 1c) present that the exterior of the hollow microsphere is composed of numerous randomly assembled nanoplates. A transmission electron microscopy (TEM) image in Fig. 1d clearly displays the loose and porous structures of the products. The HRTEM image taken on the marked part of Fig. 1d is presented in Fig. 1e. Obviously, most of the crystal lattices of primary particles are continuous. However, some discontinuous

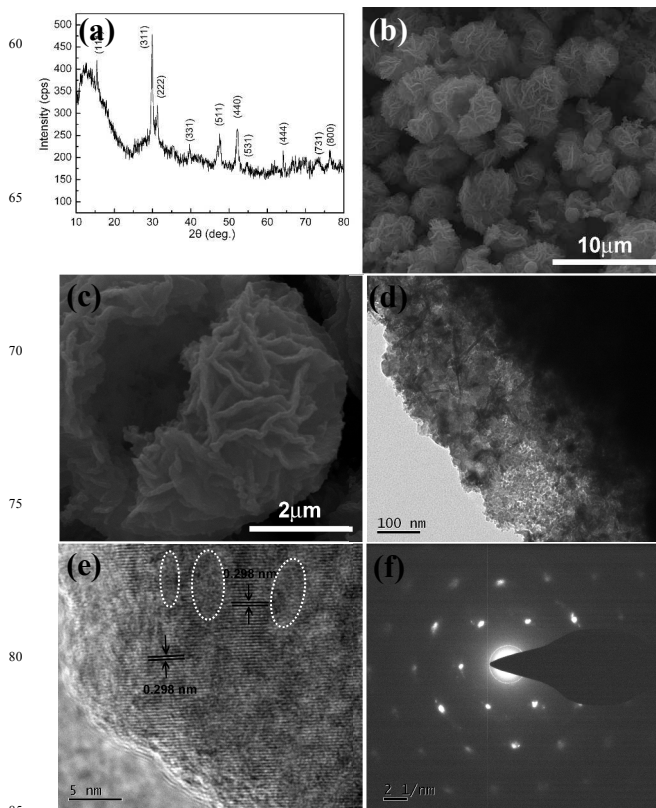


Fig. 1 (a) XRD pattern, (b) low magnified SEM image, (c) high magnified SEM image, (d) TEM image, (e) HRTEM image, and (f) SAED pattern of Co_9S_8 hollow spheres.

areas circled by white dotted line can also be observed, which should be boundaries among nanoparticles. The lattice spacings of 0.298 nm correspond to the (311) planes of Co_9S_8 . The corresponding selected-area electron diffraction (SAED) pattern is shown in Fig. 1f. The appearance of periodic diffraction spots demonstrates that all of the nanoplates in the selected area have self-assembled into highly oriented aggregates and diffract as a single crystal. Meanwhile, the misorientations deviating from perfect alignment between nanocrystallites can be reflected clearly by the elongated diffraction spots in the SAED pattern. These results indicate that the obtained nanoplates are typical mesocrystals. Similar phenomenon can be observed in the YF_3 ,¹⁶ CaCO_3 ,¹⁷ and TiO_2 ¹⁸ mesocrystals.

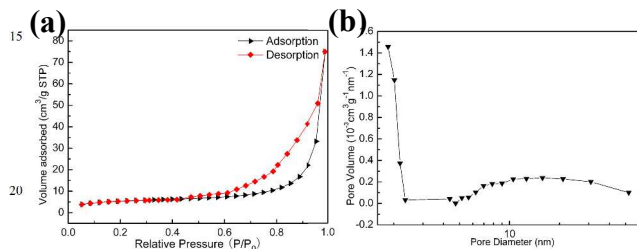


Fig. 2 The nitrogen gas adsorption-desorption isotherm loop (a) and pore size distribution (b) of Co_9S_8 hollow spheres.

Nitrogen isothermal adsorption measurement was carried out to evaluate the pore structure and the BET surface area. The N_2 adsorption-desorption isotherm at 77K and adsorption pore size distribution plot of as-prepared Co_9S_8 can be observed in Fig. 2. It can be seen the sample displays a type IV isotherm with a typical H3 hysteresis loop ($0.5 < P/P_0 < 1$), which suggests its uniform mesoporous feature (2-50 nm). The pore-size distribution in Fig. 2b further confirmed the mesoporous characterization of the product. The BET surface area of the Co_9S_8 hollow spheres is about $52.6 \text{ m}^2 \text{ g}^{-1}$.

Fig. S1 shows the cyclic voltammetry (CV) curves for the $\text{Li}/\text{Co}_9\text{S}_8$ cells. A small peak exists at around 1.75 V and two large current peaks appear at around 1.49 V and 0.32 V during discharging. Meanwhile, three oxidation peaks at 1.05, 1.89 and 2.2 V are observed in the first potential scanning cycle. Similar result can be obtained for Co_9S_8 nanoparticles.¹⁹ Co_9S_8 is transformed to an intermediate phase at 1.75 V and then converted to Co at 1.49 V. The peak appears at 0.32 V may be attributed to the formation of SEI film on the surface of electrodes, which becomes weak at subsequent cycles. Based on the above discussion, the overall charge-discharge reaction of Co_9S_8 may be explained in following way¹⁹:



After the first scan, the oxidation peaks are shifted to 1.05, 1.91 and 2.40 V. The peak current decreased very fast as the cycle numbers increased.

Fig. 3a presents the charge-discharge voltage profiles of the Co_9S_8 hollow spheres for the first, second, fifth and tenth cycles at a current density of 100 mA g^{-1} with the voltage ranging from 0.01 to 3.0 V. A high discharge capacity of $1103.9 \text{ mAh g}^{-1}$ is delivered in the 1st Li intercalation process. And a corresponding charge capacity is measured to be 838.1 mAh g^{-1} , which leads to a coulombic efficiency of 75.9%. The low initial coulomb

efficiency and the large irreversible capacity loss in the first cycle may be ascribed to the formation of solid-electrolyte interphase (SEI) film onto the surface of the electrode materials.^{7, 20} In the subsequent cycles, capacity fading can be observed. The cycle performance of the as-prepared Co_9S_8 hollow spheres between 0.01-3.0 V is shown in Fig. 3b. The obvious capacity fading in the first ten cycles may be caused by the complicated side reactions and irreversible structure transformation.^{7, 21} After 100 cycles at 100 mA g^{-1} , the discharge capacity still delivers about 254.9 mAh g^{-1} , exhibiting good charge/discharge cycling stability. To further test the cyclic stability of the anodes, the rate capability of the Co_9S_8 hollow spheres is performed. At a current density of 50 mA g^{-1} , the Co_9S_8 sample demonstrates a 10th cycle specific capacity of 876.9 mAh g^{-1} , which is higher than the theoretical capacity of Co_9S_8 (539 mAh g^{-1}).²² In addition, the reversible capacity of the sample decreases with the increasing

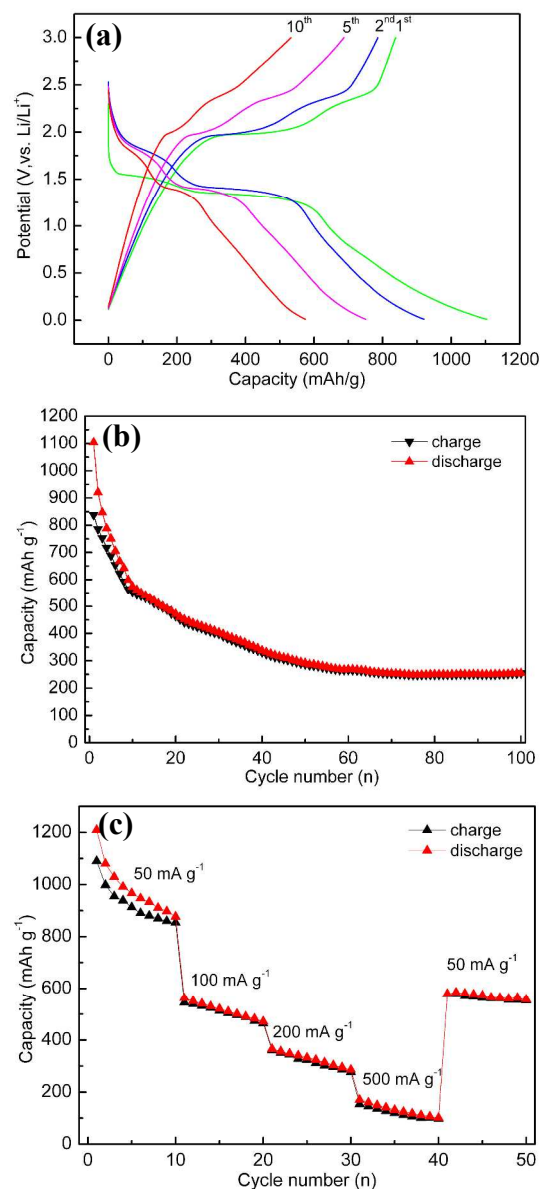


Fig. 3 (a) Charge-discharge voltage profiles, (b) cycling performance, and (c) rate performance of the hierarchical Co_9S_8 hollow spheres.

current density. The specific capacity is still remains 100.5 mAh

g^{-1} even at a high rate of 500 mA g^{-1} . If the current density reduces back to 50 mA g^{-1} , the capacity can be recovered to 557.2 mAh g^{-1} after 50 cycles. These hierarchical hollow spheres, assembled by nanoplates (mesocrystals), exhibit the higher capacity and better stability compared to those of rose-like Co_9S_8 ,¹³ Co_9S_8 nanoparticles¹⁹ and hollow microstructures.⁹ For instance, the reported Co_9S_8 hollow microstructures display specific capacity of 910.4 mAh g^{-1} at a current density of 50 mA g^{-1} . The rose-like Co_9S_8 presents a relatively poor cycling stability with the specific capacity decreased from 1051.05 to $123.04 \text{ mAh g}^{-1}$ after 30 cycles at a current density of 50 mA g^{-1} . In this case, the Co_9S_8 hollow spheres are composed of nanoplates. Such structures can effectively shorten the Li^+ diffusion length of charge carriers, resulting in the high specific capacity. Furthermore, the hollow and mesocrystalline structure can promote the penetration of electrolyte into the electrode and mitigate the volume change generated during the charge/discharge process, leading to the good cycling stability.

Conclusions

In summary, hierarchical Co_9S_8 hollow spheres self-assembled from mesocrystalline nanoplates have been fabricated via a facile solvothermal method with the help of hexamethylenetetramine. Such well-defined structure with large BET surface area, can effectively shorten the diffusion path of Li^+ and electrons during the charge/discharge process, resulting in the good Li ion storage performance. They could deliver a high capacity of 254.9 mAh g^{-1} over 100 cycles at the current density of 100 mA g^{-1} . Our results suggest that the mesocrystal materials used as anode materials have promising applications in high energy and high power lithium ion batteries.

Acknowledgments

This work was supported by the Natural Science Foundation of China (Project no. 21301086), Natural Science Foundation of Shandong Province (Project no. ZR2013BQ008), and Talent Introduction Fund of Ludong University (Project no. LY2013014).

Notes and references

a School of Chemistry & Materials Science, Ludong University, Yantai 264025, P. R. China. E-mail: jinrc427@126.com; Fax: +86 535 6696162; Tel: +86 535 6696162

b Department of Chemistry, Harbin Institute of Technology, Harbin 150001, P. R. China.

† Electronic Supplementary Information (ESI) available: [details of any supplementary information available should be included here]. See DOI: 10.1039/b000000x/

‡ Footnotes should appear here. These might include comments relevant to but not central to the matter under discussion, limited experimental and spectral data, and crystallographic data.

1. J. W. Fergus, *J Power Sources*, 2010, **195**, 939-954.
2. J. Zhang, T. Huang, Z. Liu and A. Yu, *Electrochem. Commun.*, 2013, **29** 17-20.
3. L. Ji, Z. Lin, M. Alcoutlabia and X. Zhang, *Energy Environ. Sci.*, 2011, **4**, 2682-2699.

4. L. Ji, O. Toprakci, M. Alcoutlabi, Y. Yao, Y. Li, S. Zhang, B. Guo, Z. Lin and X. Zhang, *ACS Appl. Mater. Interfaces*, 2012, **4** 2672-2679.
5. L. Ji, H. L. Xin, T. R. Kuykendall, S.-L. Wu, H. Zheng, M. Rao, E. J. Cairns, V. Battaglia and Y. Zhang, *Phys. Chem. Chem. Phys.*, 2012, **14**, 6981-6986.
6. Q. H. Wang, L. F. Jiao, H. M. Du, W. X. Peng, Y. Han, D. W. Song, Y. C. Si, Y. J. Wang and H. T. Yuan, *J. Mater. Chem.*, 2011, **21**, 327-329.
7. Q. H. Wang, L. F. Jiao, Y. Han, H. M. Du, W. X. Peng, Q. N. Huan, D. W. Song, Y. C. Si, Y. J. Wang and H. T. Yuan, *J. Phys. Chem. C*, 2011, **115**, 8300-8304.
8. N. Mahmood, C. Zhang, J. Jiang, F. Liu and Y. Hou, *Chem. Eur. J.*, 2013, **19**, 5183-5190.
9. Y. X. Zhou, H. B. Yao, Y. Wang, H. L. Liu, M. R. Gao, P. K. Shen and S. H. Yu, *Chem. Eur. J.*, 2010, **16**, 12000-12007.
10. M. He, L. Yuan, X. Hu, W. Zhang, J. Shu and Y. Huang, *Nanoscale*, 2013, **5**, 3298-3305.
11. K. Brezesinski, J. Haetge, J. Wang, S. Mascotto, C. Reitz, A. Rein, S. H. Tolbert, J. Perlich, B. Dunn and T. Brezesinski, *Small*, 2011, **7**, 407-414.
12. J. Zhu, Z. Yin, D. Yang, T. Sun, H. Yu, H. E. Hoster, H. H. Hng, H. Zhang and Q. Yan, *Energy Environ. Sci.*, 2013, **6**, 987-993.
13. R. Jin, J. Liu, Y. Xu, G. Li and G. Chen, *J. Mater. Chem. A*, 2013, **1**, 7995-7999.
14. S. Jin, H. Deng, D. Long, X. Liu, L. Zhan, X. Liang, W. Qiao and L. Ling, *J. Power Sources*, 2011 **196**, 3887-3893.
15. L. Ji, Z. Lin, A. J. Medford and X. Zhang, *Carbon*, 2009, **47**, 3346-3354.
16. S.-L. Zhong, Y. Lu, M.-R. Gao, S.-J. Liu, J. Peng, L.-C. Zhang and S.-H. Yu, *Chem. Eur. J.*, 2012, **18**, 5222 - 5231.
17. X. Geng, L. Liu, J. Jiang and S.-H. Yu, *Cryst. Growth Des.*, 2010, **10**, 3448-3453.
18. S.-J. Liu, J.-Y. Gong, B. Hu and S.-H. Yu, *Cryst. Growth Des.*, 2008, **9**, 203-209.
19. J. Wang, S. H. Ng, G. X. Wang, J. Chen, L. Zhao, Y. Chen and H. K. Liu, *J. Power Sources*, 2006, **159**, 287-290.
20. Y. Gu, Y. Xu and Y. Wang, *ACS Appl. Mater. Interfaces*, 2013, **5**, 801-806.
21. J. Z. Zhao, Z. L. Tao, J. Liang and J. Chen, *Cryst. Growth Des.*, 2008, **8** 2799-2805.
22. J. M. Yan, H. Z. Huang, J. Zhang, Z. J. Liu and Y. Yang, *J. Power Sources*, 2005, **146**, 264-269.

TOC

Mesocrystal Co_9S_8 hollow spheres are reported through a convenient preparation route, and exhibit good performance for Li-ion batteries.

